Supporting Information

for

An ESIPT-active Orange-emissive 2-(2′-Hydroxyphenyl)imidazo[1,2-a]pyridine-derived Chemodosimeter for Turn-on Detection of Fluoride Ions via Desilylation

Akhil A. Bhosle, Mainak Banerjee,* Ankit Thakuri, Pooja D. Vishwakarma and Amrita Chatterjee*

Department of Chemistry, Birla Institute of Technology and Science Pilani, KK Birla Goa Campus, Goa 403726, India.

*E-mail: mainak@goa.bits-pilani.ac.in; amrita@goa.bits-pilani.ac.in.

Table of Contents

1. UV-Vis response of HIP-Br in different solvents

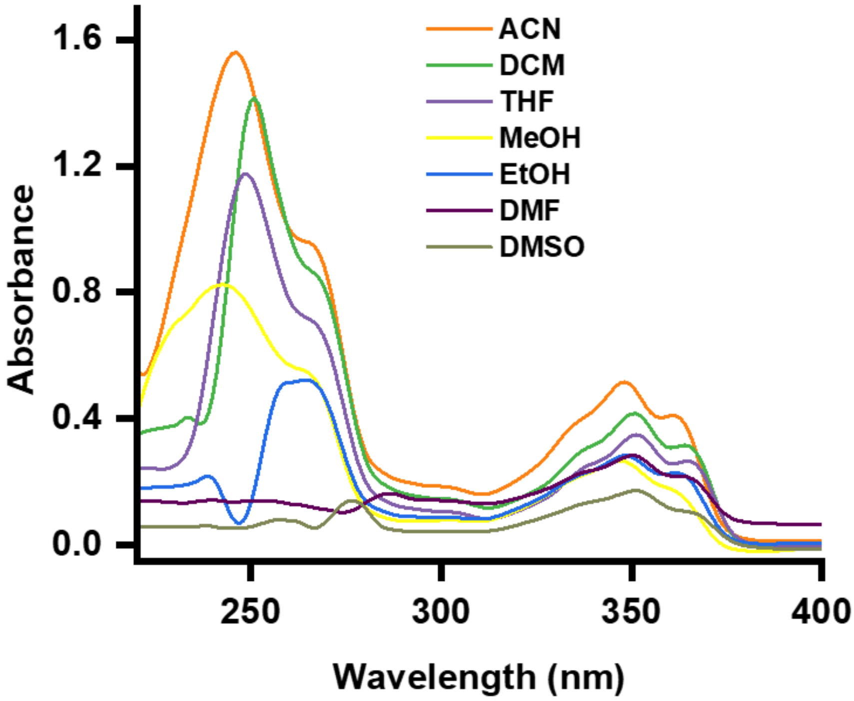

Figure S1. The UV-Vis responses of **HIP-Br** (30 µM) in different solvents showing the absorption band at around 340 nm along with a shoulder band at around 360 nm.

2. Fluorescence response of HIP-Br in water-THF fractions

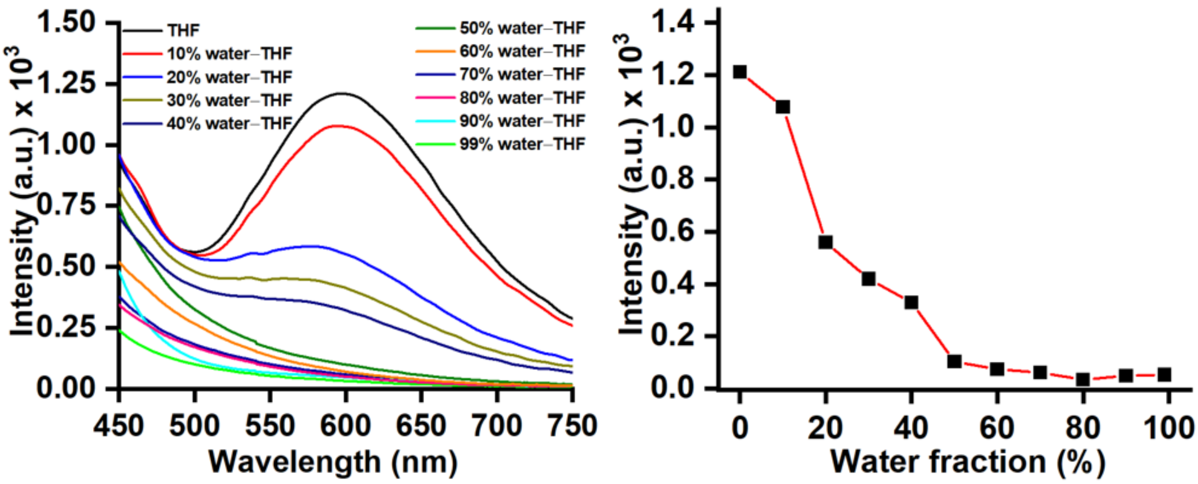

Figure S2. The fluorescence responses of **HIP-Br** (10 µM) at 598 nm as a function of different water–THF fractions (%f_w) showing a decrease in emission with the increase in water fractions.

3. Table S1: Comparative photophysical studies of HIP-Br and HBT-Br

Solvent	λ_{abs1} (nm)	λ_{abs2} (nm)	λ_{em1} (nm)	Int.	λ_{em2} (nm)	Int.	Stokes shift (nm)	φ_1	φ_2
DCM	290	348	-	-	523	2585	175	-	4.6
THF	295	345	-	-	535	831	190	-	1.25
ACN	293	345	-	-	538	481	193	-	0.6
DMF	292	342	466	5495	-	-	124	10.7	-
DMSO	292	342	468	5805	-	-	126	11.02	-
EtOH	-	341	429	8758	-	-	88	25.2	-
MeOH	291	340	427	5100	-	-	87	5.4	-

4. UV-Vis and fluorescence spectra of HIPS-Br and HIP-Br

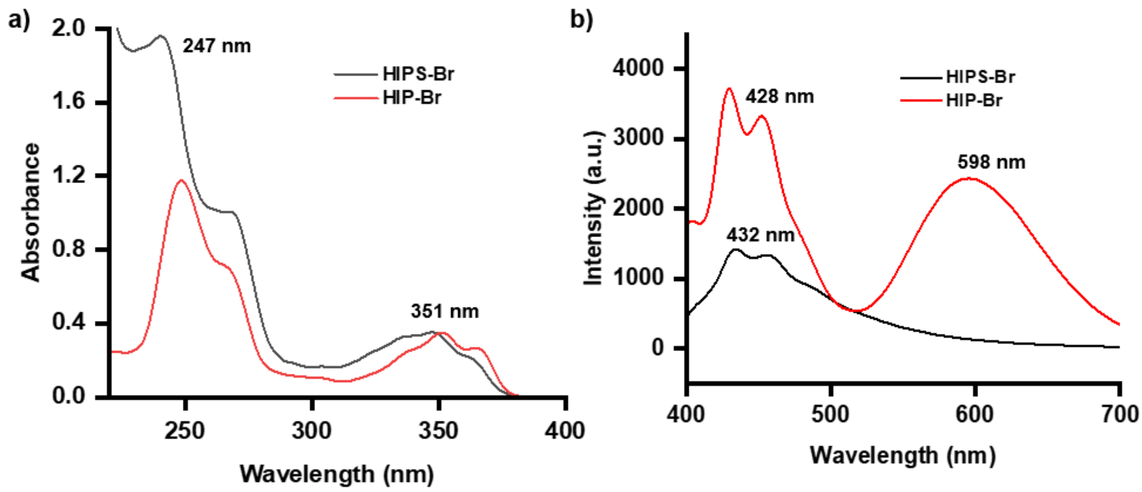

Figure S3. a) UV-Vis and b) fluorescence spectra of **HIPS-Br** and **HIP-Br** in THF.

5. Fluorescence response of HIP-Br and HIPS-Br at different pH ranges

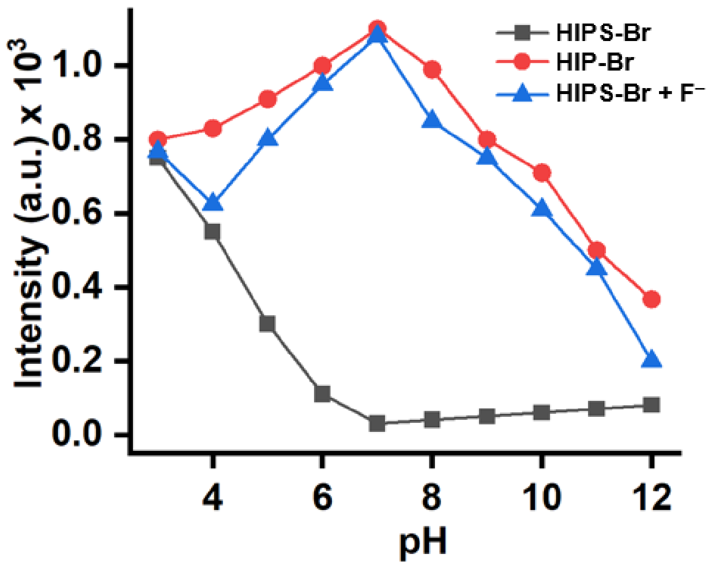

Figure S4. The fluorescence responses of **HIPS-Br** and **HIP-Br** in the presence and absence of F^- ions at 598 nm as a function of pH.

6. Fluorescence response of HIPS-Br in water-THF fractions

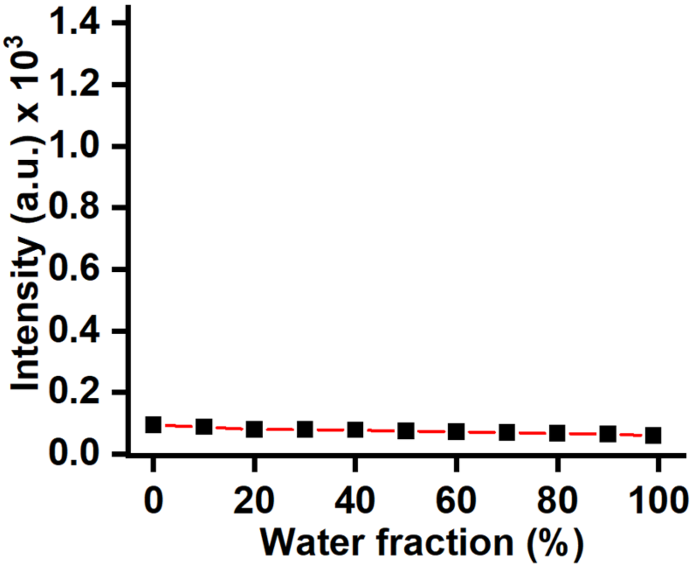

Figure S5. The fluorescence responses of **HIPS-Br** (10 μM) at 598 nm as a function of different water–THF fractions (%f_w) showing a turn-off response due to restriction in intramolecular proton transfer.

7. Time-dependent study for HIPS-Br upon addition of F^-

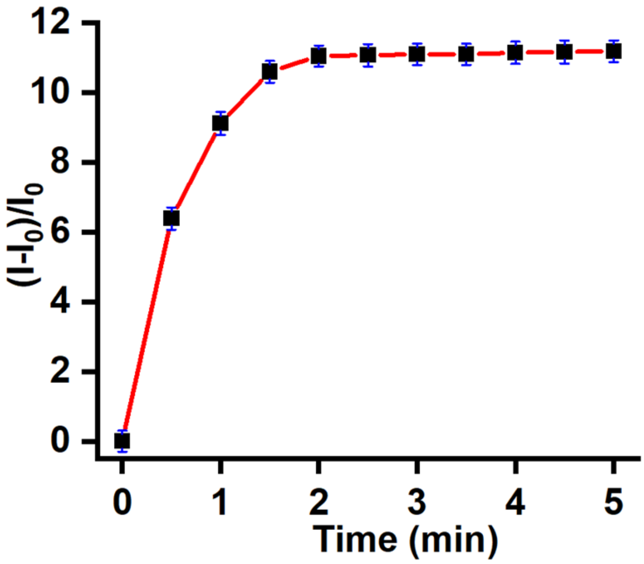

Figure S6. Time-dependent study and effect on the relative emission intensities of **HIPS-Br** (10 μM) upon addition of 60 μM of F^- ions (λ_{ex} 350 nm; λ_{em} 598 nm).

8. Fluorence spectra HIPS-Br before and after the addition of F^-

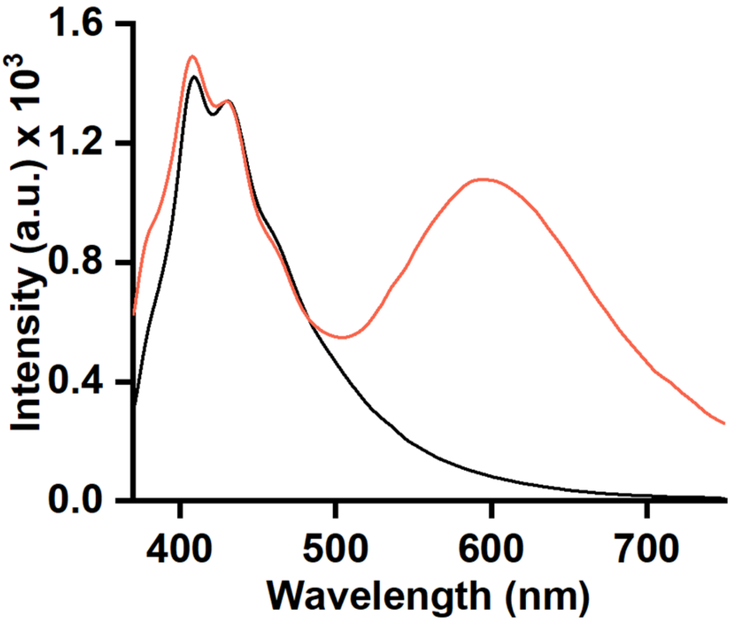

Figure S7. Fluorescence response of **HIPS-Br** (10 µM in water–THF (1:9)) before (black) and after (red) the addition of F^- ions indicating no change in the emission at 410 nm (λ_{ex} 350 nm; λ_{em} 598 nm).

9. UV-Vis responses of HIPS-Br in the presence and absence of F^- ions

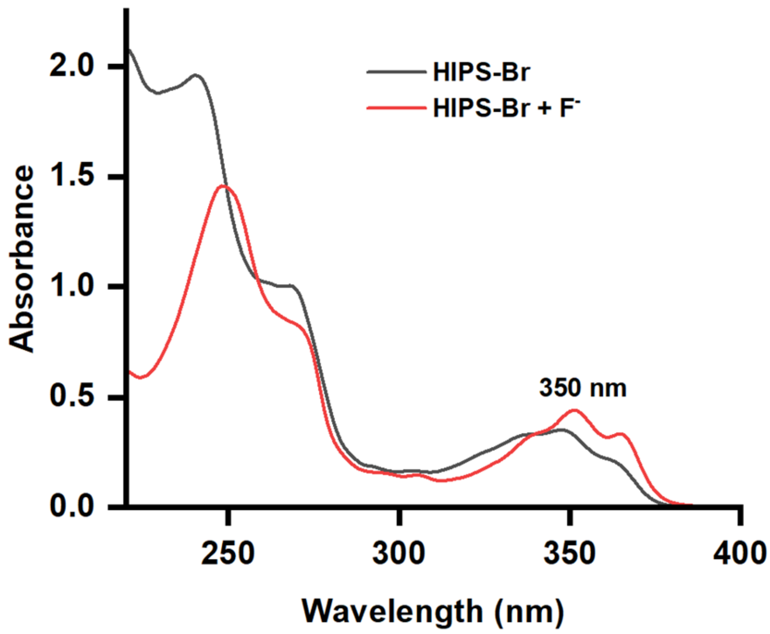

Figure S8. The UV-Vis responses of **HIPS-Br** (30 µM) in the presence and the absence of F^- ions (80 µM) showed no significant change in the absorption band at 350 nm.

10. Comparison of the present study with ESIPT-based and silyl cleavage-based detection of fluoride

Sr. No.	Probe Structure	Response	Linear range (µM)	Detection limit (nm)	Real sample analysis	Solid- phase study	Ref.
	ESIPT-based						
1.	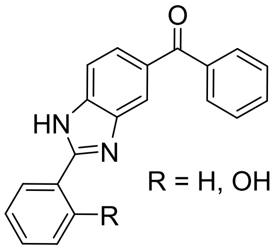 λ_{ex} = 360 nm, λ_{em1} = 420 nm, λ_{em2} = 540 nm	ratiometric	2-2.4 x 10^3	2.0 x 10^3	-	TLC strips	1
2.	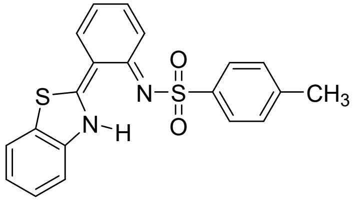 λ_{ex} = 370 nm, λ_{em} = 540 nm	turn-on	0-50	2.9 x 10^3	-	-	2
3.	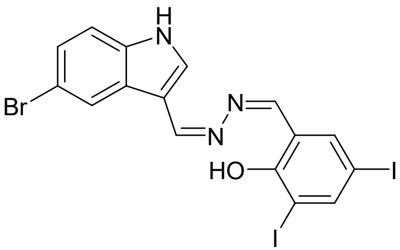	turn-on	0-50	120	detection in HeLa cells	-	3

	$\lambda_{ex} = 360$ nm, $\lambda_{em} = 430$ nm						
4.	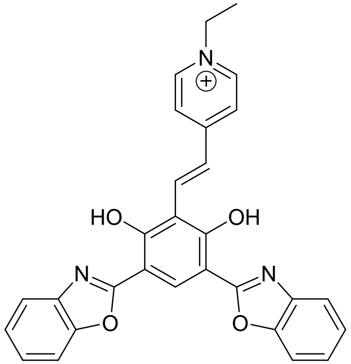 $\lambda_{ex} = 535$ nm, $\lambda_{em1} = 720$ nm, $\lambda_{em2} = 450$ nm	ratiometric	1-10	1×10^3	-	-	4
5.	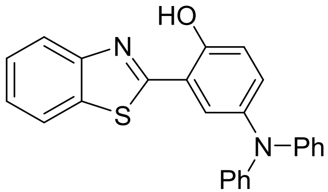 $\lambda_{ex} = 365$ nm, $\lambda_{em} = 530$ nm,	turn-on	-	11	-	filter paper	5
	Silyl cleavage based						
6.	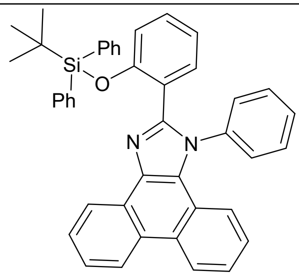	ratiometric	0-2	430	-	-	6

	λ_{ex} = 322 nm, λ_{em1} = 384 nm, λ_{em2} = 475 nm						
7.	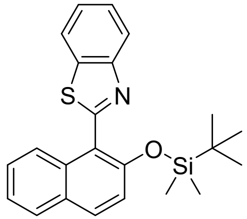 λ_{ex} = 350 nm, λ_{em1} = 407 nm, λ_{em2} = 477 nm	ratiometric	-	6.5 x 10^3	analysis in HeLa cells	paper strips	7
8.	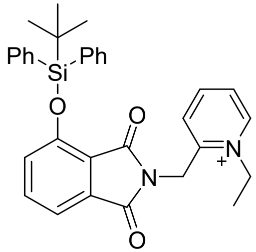 λ_{ex} = 413 nm, λ_{em} = 511 nm	turn-on	0-70	1.16 x 10^3	-	-	8
9.	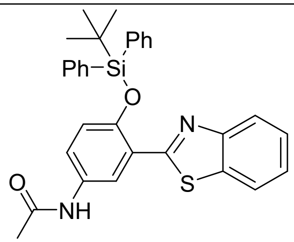 λ_{ex} = 345 nm, λ_{em1} = 406 nm, λ_{em2} = 494 nm	ratiometric	25-200	25 x 10^3	-	hydrogel	9

10.	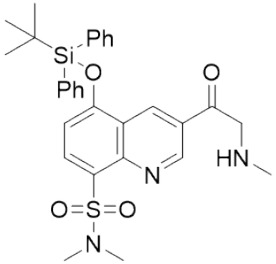 λ_{ex} = 346 nm, λ_{em1} = 553 nm	turn-on	0-200	50 x 10^3	-	paper strips	10
11.	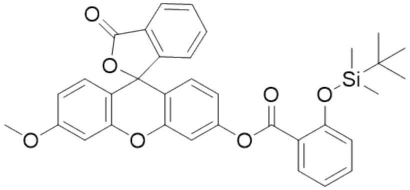 λ_{ex} = 460 nm, λ_{em1} = 523 nm	turn-on	-	1.03 x 10^3	detection in HeLa cells	-	11
12.	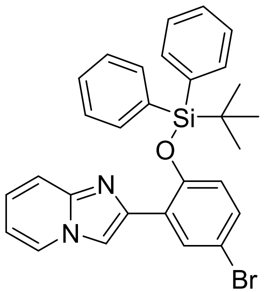 λ_{ex} = 350 nm, λ_{em1} = 598 nm	turn-on	1-10	66	water samples and toothpaste	TLC strips	This work

11. References

1. A. S. Gupta, K. Paul and V. Luxami, Ratiometric fluorescent chemosensor for fluoride ion based on inhibition of excited state intramolecular proton transfer. *Spectrochim. Acta, Part A*, 2015, **138**, 67−72. https://doi.org/10.1016/j.saa.2014.11.026
2. G. Dhaka, N. Kaur and J. Singh, Exploiting the INHIBIT-ESIPT mechanism for the design of fluorescent chemosensor with a large blue-shift in emission. *J. Photochem. Photobiol., A*, 2017, **335**, 174−181. https://doi.org/10.1016/j.jphotochem.2016.11.018
3. K. Karuppiah, M. Nelson, M. M. Alam, M. Selvaraj, M. Sepperumal and S. Ayyanar, A new 5-bromoindolehydrazone anchored diiodosalicylaldehyde derivative as efficient fluoro and chromophore for selective and sensitive detection of tryptamine and F− ions: Applications in live cell imaging. *Spectrochim. Acta, Part A*, 2022, **269**, 120777. https://doi.org/10.1016/j.saa.2021.120777
4. C. S. Abeywickrama and Y. Pang, Synthesis of a bis[2-(2′-hydroxyphenyl)benzoxazole]pyridinium derivative: The fluoride-induced large spectral shift for ratiometric response. *New J. Chem.*, 2021, **45**, 9102–9108. https://doi.org/10.1039/D1NJ00044F
5. H. Dai, H. Zeng, H. Li, J. Long, K. W. Ng, Y. Wang, B. Xu, G. Shi, Z. Chi and C. Liu, Manipulation of excited-state intramolecular proton transfer by electron-donor substitution for high performance fluoride ions sensing. *Spectrochim. Acta, Part A*, 2024, 306, 123530. https://doi.org/10.1016/j.saa.2023.123530.
6. X. Li, B. Hu, J. Li, P. Lu and Y. Wang, Fluoride anion detection based on the excited state intramolecular proton transfer (ESIPT) of 2-(o-hydroxyphenyl)imidazole induced by the Si–O cleavage of its silyl ether. *Sens. Actuators, B*, 2014, **203**, 635−640. https://doi.org/10.1016/j.snb.2014.07.014
7. S. Goswami, A. K. Das, A. Manna, A. K. Maity, H. K. Func, C. K. Quah and P. Saha, A colorimetric and ratiometric fluorescent turn-on fluoride chemodosimeter and application in live cell imaging: High selectivity via specific Si-O cleavage in semi aqueous media and prompt recovery of ESIPT along with the X-ray structures. *Tetrahedron Lett.*, 2014, **55**, 2633 −2638. https://doi.org/10.1016/j.tetlet.2014.03.003
8. X. Liu, X. Liu, Y. Shen and B. Gu, A simple water-soluble ESIPT fluorescent probe for fluoride ion with large stokes shift in living cells. *ACS Omega*, 2020, **5**, 21684−21688. https://doi.org/10.1021/acsomega.0c02589

9. L. Xiong, J. Feng, R. Hu, S. Wang, S. Li, Y. Li and G. Yang, Sensing in 15 s for aqueous fluoride anion by water-insoluble fluorescent probe incorporating hydrogel. *Anal. Chem.*, 2013, **85**, 4113–4119. https://doi.org/10.1021/ac400252u
10. X. Q. Zhou, R. Lai, H. Li and C. I. Stains, The 8-silyloxyquinoline scaffold as a versatile platform for the sensitive detection of aqueous fluoride. *Anal. Chem.*, 2015, **87**, 4081–4086. https://doi.org/10.1021/acs.analchem.5b00430
11. A. Roy, D. Kand, T. Saha and P. Talukdar, A cascade reaction based fluorescent probe for rapid and selective fluoride ion detection. *RSC Adv.*, 2014, **4**, 33890–33896 https://doi.org/10.1039/C4CC01665C

12. NMR Spectra:

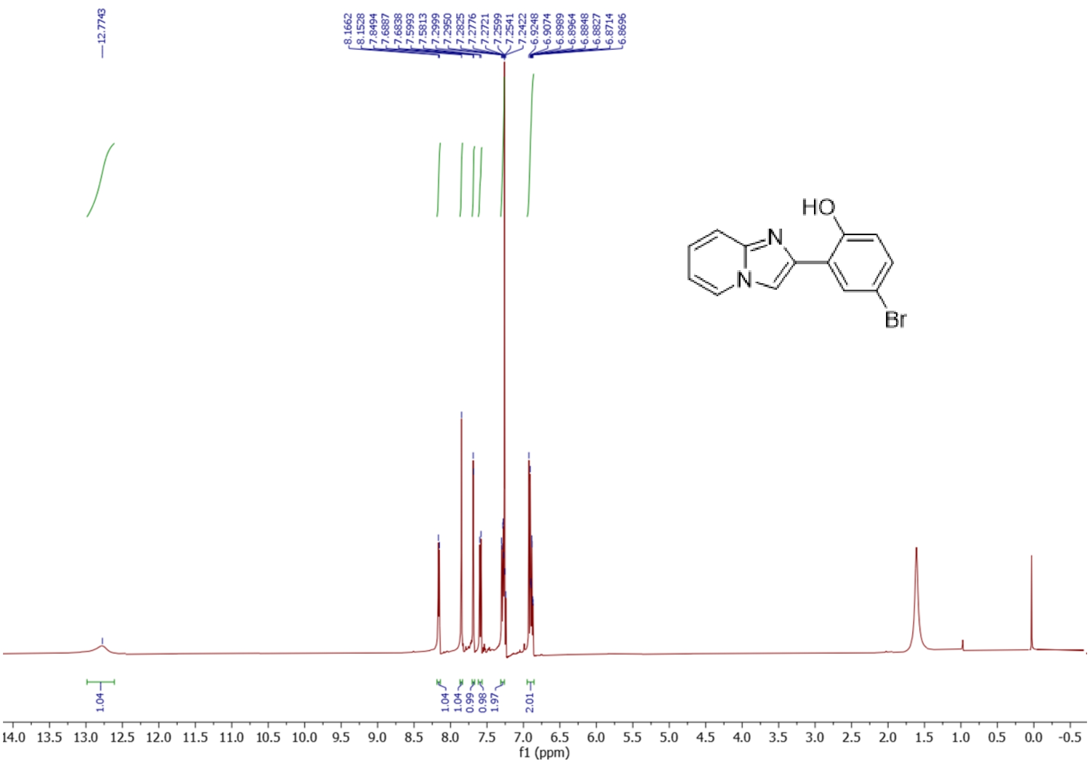

^{1}H NMR spectrum of 4-bromo-2-(imidazo[1,2-*a*]pyridin-2-yl)phenol (**HIP-Br**) ($CDCl_3$, 500 MHz).

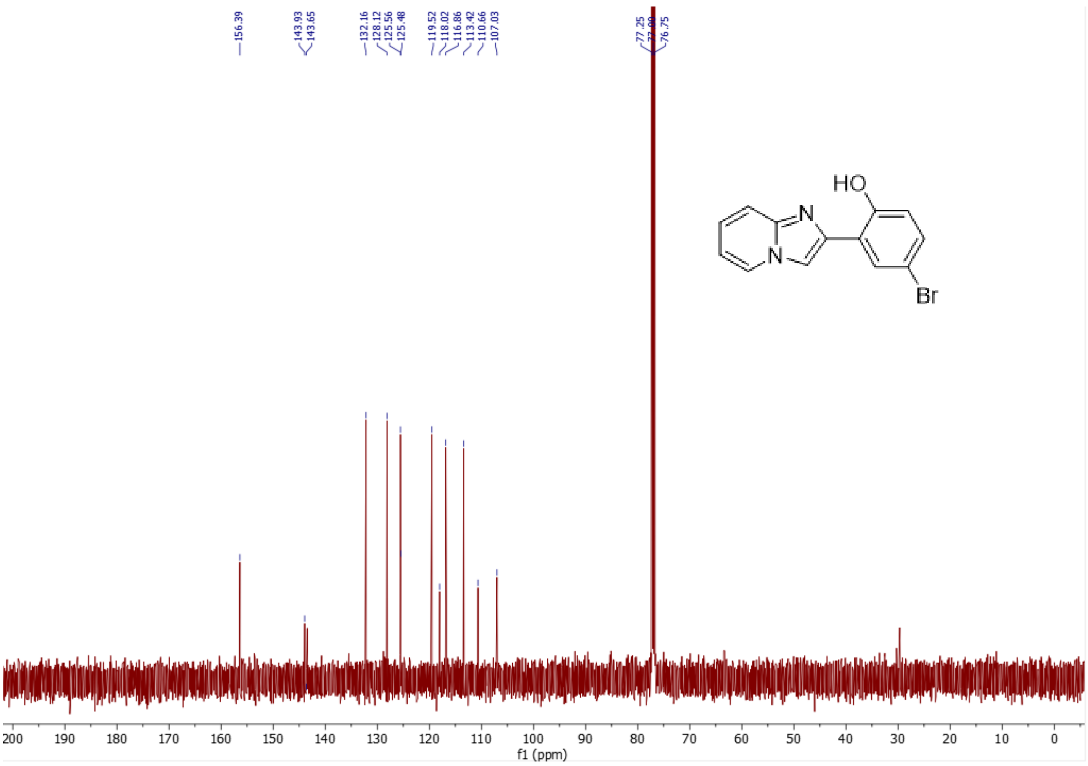

^{13}C NMR spectrum of 4-bromo-2-(imidazo[1,2-*a*]pyridin-2-yl)phenol (**HIP-Br**) ($CDCl_3$, 125 MHz).

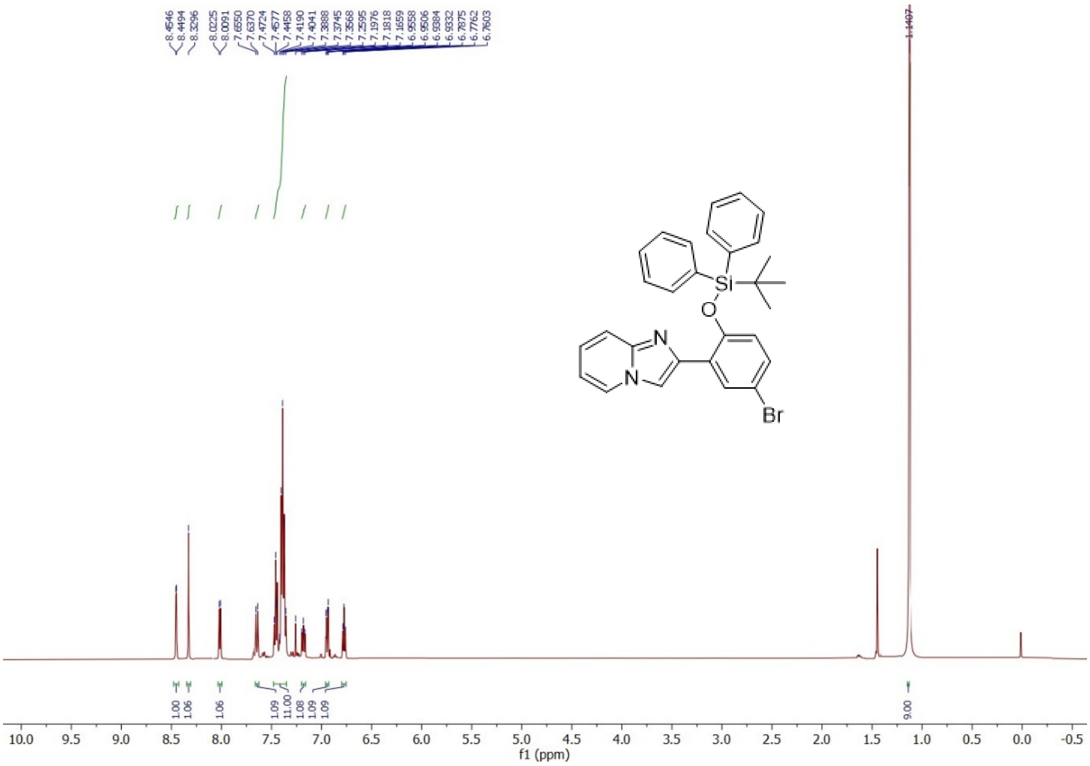

[1]H NMR spectrum of 2-(5-bromo-2-((*tert*-butyldiphenylsilyl)oxy)phenyl)imidazo[1,2-*a*]pyridine (**HIPS-Br**) ($CDCl_3$, 500 MHz).

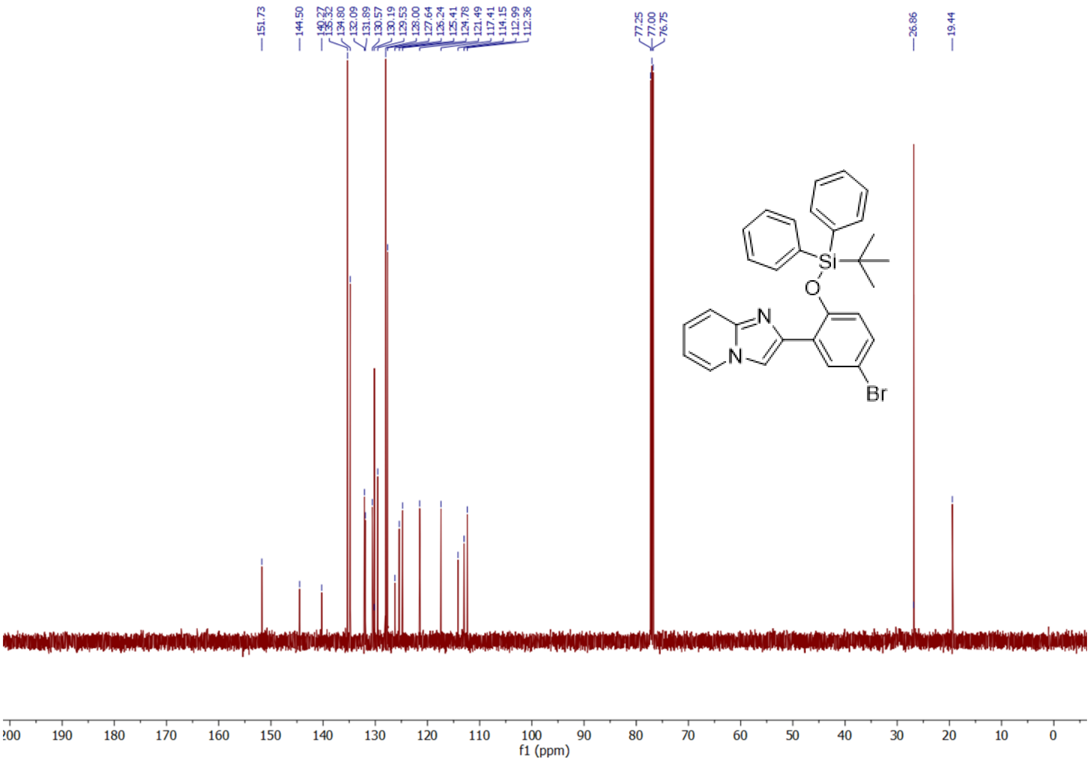

[13]C NMR spectrum of 2-(5-bromo-2-((*tert*-butyldiphenylsilyl)oxy)phenyl)imidazo[1,2-*a*]pyridine (**HIPS-Br**) ($CDCl_3$, 125 MHz).

13. Simulated input structure and coordinates

Input coordinates of HIPS-Br ($SiC_{29}N_2H_{27}OBr$)

C	-1.501157000	6.054280000	0.104559000
C	-0.113891000	5.803478000	0.151104000
C	0.348008000	4.477931000	0.155631000
N	-0.568107000	3.477782000	0.114245000
C	-1.889546000	3.692461000	0.070019000
C	-2.410307000	4.983473000	0.063343000
C	-0.393506000	2.150080000	0.107939000
C	-1.660010000	1.560947000	0.056446000
N	-2.595414000	2.546875000	0.034767000
C	-2.024302000	0.107281000	0.027222000
C	-3.394024000	-0.228154000	0.014895000
C	-3.805085000	-1.559037000	-0.010537000
C	-2.858856000	-2.576956000	-0.024160000
C	-1.498923000	-2.271393000	-0.015002000
C	-1.056856000	-0.938649000	0.008468000
O	0.259353000	-0.608351000	0.014034000
Br	-5.666997000	-1.985304000	-0.024305000
Si	1.884504000	-1.184499000	-0.053981000
C	2.601864000	-0.252366000	-1.514282000
C	2.637401000	-0.536360000	1.535858000
C	2.219056000	-3.081978000	-0.245005000
C	1.727539000	-3.830541000	1.013196000
C	1.558458000	-3.597417000	-1.541781000
C	3.725679000	-3.391931000	-0.373587000
C	4.021081000	-0.588288000	1.776301000
C	4.549953000	-0.093487000	2.972387000
C	3.706093000	0.457817000	3.937844000
C	2.330832000	0.517428000	3.708606000
C	1.796918000	0.024642000	2.514565000
C	3.982456000	-0.240364000	-1.776978000
C	4.487989000	0.469582000	-2.870300000
C	3.623648000	1.173958000	-3.709988000
C	2.251127000	1.170914000	-3.457414000
C	1.740494000	0.463149000	-2.365756000
H	-1.866112000	7.073077000	0.100559000
H	0.588618000	6.626004000	0.182929000
H	1.408116000	4.259582000	0.190693000
H	-3.477905000	5.157737000	0.027291000
H	0.577388000	1.684401000	0.140273000
H	-4.149795000	0.546990000	0.026752000
H	-3.176772000	-3.611698000	-0.042344000
H	-0.819681000	-3.082588000	-0.024748000
H	0.668273000	-3.675367000	1.252525000
H	2.292645000	-3.485464000	1.906100000
H	1.893020000	-4.924434000	0.906554000
H	0.476526000	-3.420543000	-1.598947000
H	1.727145000	-4.689686000	-1.659275000
H	1.999498000	-3.085705000	-2.424660000
H	4.288364000	-3.079707000	0.525192000

H	4.164786000	-2.920115000	-1.273061000
H	3.888056000	-4.486801000	-0.482130000
H	4.698232000	-0.999158000	1.049790000
H	5.616935000	-0.136349000	3.149633000
H	4.118182000	0.840190000	4.862817000
H	1.676539000	0.945765000	4.456927000
H	0.727777000	0.080521000	2.361328000
H	4.674458000	-0.766620000	-1.143181000
H	5.552768000	0.474932000	-3.065032000
H	4.017659000	1.723071000	-4.555342000
H	1.580906000	1.717554000	-4.108161000
H	0.673229000	0.474229000	-2.192959000

Input coordinates of HIP-Br ($C_{13}N_2H_9OBr$)

N	-0.202689000	0.709307000	0.008319000
C	-0.291626000	-0.682871000	-0.004828000
C	0.880783000	-1.452867000	0.020595000
C	2.126258000	-0.758892000	0.059298000
C	2.184433000	0.635865000	0.071643000
C	0.999464000	1.401364000	0.045847000
C	-1.509932000	1.210269000	-0.022797000
C	-2.378570000	0.073828000	-0.054836000
N	-1.620454000	-1.068031000	-0.043374000
C	-3.816899000	0.030437000	-0.093670000
C	-4.472116000	-1.232336000	-0.120973000
C	-5.850439000	-1.302696000	-0.158409000
C	-6.657556000	-0.160325000	-0.171178000
C	-6.028841000	1.093675000	-0.144653000
C	-4.639944000	1.189270000	-0.106738000
O	-4.001950000	2.434548000	-0.080032000
Br	-6.710358000	-3.053175000	-0.194960000
H	0.812009000	-2.530103000	0.010423000
H	3.045929000	-1.333423000	0.079469000
H	3.136699000	1.150227000	0.101108000
H	0.952538000	2.479743000	0.052933000
H	-1.734597000	2.260738000	-0.020685000
H	-3.860919000	-2.124396000	-0.111511000
H	-7.736066000	-0.240932000	-0.200668000
H	-6.631713000	1.998238000	-0.153795000
H	-4.649841000	3.164139000	-0.091728000

Input coordinates of HIP-Br$_{IPT}$ ($C_{13}N_2H_9OBr$)

C	5.557682000	-0.432946000	0.215505000
C	5.095813000	-1.714656000	-0.133084000
C	3.724490000	-1.921513000	-0.325686000
N	2.882967000	-0.868671000	-0.167439000
C	3.285540000	0.365192000	0.164866000
C	4.651265000	0.628600000	0.369557000
C	1.551884000	-0.828606000	-0.294136000
C	1.119670000	0.478798000	-0.034539000

N	2.239484000	1.230779000	0.256459000
C	-0.360115000	0.865953000	-0.050812000
C	-1.313389000	-0.186939000	0.011700000
C	-2.687067000	0.063736000	0.009015000
C	-3.158469000	1.366982000	-0.058789000
C	-2.260067000	2.423431000	-0.128215000
C	-0.877805000	2.195397000	-0.127488000
O	-0.088982000	3.264554000	-0.233924000
Br	-3.923319000	-1.390322000	0.102945000
H	6.616322000	-0.264146000	0.365123000
H	5.793502000	-2.533294000	-0.251522000
H	3.345856000	-2.900192000	-0.593805000
H	5.025678000	1.604779000	0.633972000
H	0.960322000	-1.692554000	-0.559700000
H	-1.007030000	-1.217282000	0.080738000
H	-4.223161000	1.562603000	-0.061838000
H	-2.638609000	3.436421000	-0.190629000
H	2.321383000	2.193171000	0.515484000